HEALTH AND MEDICINE

Self-assembling synthetic nanoadjuvant scaffolds cross-link B cell receptors and represent new platform technology for therapeutic antibody production

Sujata Senapati[1], Ross J. Darling[2], Kathleen A. Ross[1,3], Michael J. Wannemeuhler[2,3], Balaji Narasimhan[1,3]*, Surya K. Mallapragada[1,3]*

Copyright © 2021 The Authors, some rights reserved; exclusive licensee American Association for the Advancement of Science. No claim to original U.S. Government Works. Distributed under a Creative Commons Attribution NonCommercial License 4.0 (CC BY-NC).

Host antibody responses are pivotal for providing protection against infectious agents. We have pioneered a new class of self-assembling micelles based on pentablock copolymers that enhance antibody responses while providing a low inflammatory environment compared to traditional adjuvants. This type of "just-right" immune response is critical in the rational design of vaccines for older adults. Here, we report on the mechanism of enhancement of antibody responses by pentablock copolymer micelles, which act as scaffolds for antigen presentation to B cells and cross-link B cell receptors, unlike other micelle-forming synthetic block copolymers. We exploited this unique mechanism and developed these scaffolds as a platform technology to produce antibodies in vitro. We show that this novel approach can be used to generate laboratory-scale quantities of therapeutic antibodies against multiple antigens, including those associated with SARS-CoV-2 and *Yersinia pestis*, further expanding the value of these nanomaterials to rapidly develop countermeasures against infectious diseases.

INTRODUCTION

The diversity in population demographics (as a function of age, genetics, and other factors) leads to substantial variability in the induction of host immune responses to vaccines, requiring the development of novel adjuvants. A case in point is the coronavirus disease 2019 (COVID-19) pandemic, which has, for example, disproportionately affected older adults (*1*). Efficient preventive measures for such threats require the design of vaccine adjuvants that can balance competing and complex requirements. To achieve rational design of vaccines for older adults, it is important to generate vaccine formulations that account for immunosenescence and judiciously balance the competition between the exacerbated inflammation associated with aged individuals and the induction of efficacious immune responses. Traditional adjuvants [e.g., Toll-like receptor (TLR) agonists] typically induce robust immune responses but can also exacerbate the chronic inflammatory environment, which is known to diminish immune responses in aged individuals (*2*, *3*). Because a robust B cell response is critical for providing antibody-based protection against many infectious diseases (including COVID-19) (*4*–*6*), mechanistic studies exploring the interaction of adjuvants and immunogens with B cells have important implications for the development of new and more effective vaccines.

Self-assembling micellar systems of different sizes and chemistries have been extensively used for vaccine delivery (*7*). Their small size (<100 nm), flexibility for functionalization, and ability to deliver antigens (Ag) to Ag-presenting cells (APCs) make them promising platforms for vaccine adjuvants. There are multiple reports on the use of micelle-based adjuvants (*8*–*10*). Their immune-enhancing characteristics are similar to that of the aforementioned traditional adjuvants in that they activate APCs, induce pro-inflammatory cytokine secretion, and lead to antibody responses with similar kinetics (*11*–*13*). However, little is known about their mechanism of action in the context of B cell activation, differentiation, and antibody production.

We recently reported on the synthesis of a new class of amphiphilic pentablock copolymers (PBCs) based on the U.S. Food and Drug Administration (FDA)–approved temperature-responsive (*14*) Pluronic F127 and cationic end-group blocks of poly(diethylaminoethylmethacrylate) (PDEAEM), which undergo both temperature- and pH-responsive self-assembly to form micelles (*15*). The cationic PBC micelles have been shown to associate with Ag to form PBC micelle–Ag complexes and enhance Ag delivery to APCs (*16*). They have also been demonstrated to induce rapid and short-term enhancement in antibody responses in mice (*16*). However, the underlying mechanism of action of these PBC micelles with respect to B cell activation is unknown. In addition, studies indicate that the PBC micelles neither activate APCs (e.g., cell surface marker expression) nor lead to the induction of innate effector molecules such as nitric oxide, reactive oxygen species, or pro-inflammatory cytokines (*16*). This enhanced humoral immune response induced by the PBC micelles while inducing less inflammation is especially beneficial for the development of vaccine formulations for older adults (*17*, *18*). This is because traditional adjuvants such as TLR agonists, alum, and MF59 may exacerbate chronic inflammation, which leads to diminished immune responses in aged individuals (*19*–*21*).

We hypothesize that the dissimilarity in characteristics of the immune response generated between the PBC micelles and traditional adjuvants may be attributed to the material properties of the PBC micelles and the mechanisms involved in their interactions with and activation of B cells. In this work, we delineated the mechanism underlying the Ag-specific B cell responses induced by PBC micelles and identified key attributes contributing to this behavior. By observing increased expression of Nur77 [a marker for Ag–B cell receptor (BCR) engagement], we demonstrated that cross-linking of BCRs by PBC micelles leads to B cell activation (*22*). After confirming the engagement of BCRs with the PBC micelle–Ag complexes, we show that BCR cross-linking induces B cell proliferation in vitro, leading

[1]Department of Chemical and Biological Engineering, Iowa State University, Ames, IA, USA. [2]Department of Veterinary Microbiology and Preventive Medicine, Iowa State University, Ames, IA, USA. [3]Nanovaccine Institute, Iowa State University, Ames, IA, USA.
*Corresponding author. Email: suryakm@iastate.edu (S.K.M.); nbalaji@iastate.edu (B.N.)

Downloaded from http://advances.sciencemag.org/ on August 11, 2021

to the production of Ag-specific antibodies. Last, we demonstrate that BCR cross-linking by PBC micelles can be exploited for in vitro production of therapeutic antibodies to a diverse array of Ag associated with *Yersinia pestis* (F1-V) and severe acute respiratory syndrome coronavirus 2 (SARS-CoV-2) [spike (S) protein].

RESULTS

Material characterization

The purity and molecular mass of the synthesized PBC were determined using ^{1}H nuclear magnetic resonance (NMR). The spectrum showed multiple characteristic peaks (fig. S1, A and B), consistent with previous work (*23*), and the average molecular weight was calculated to be 14,600 g/mol. The mean diameter of the PBC micelles (fig. S1C) determined using dynamic light scattering was 30.4 nm (±2.7 nm), and the zeta potential was +5.82 mV (±0.89 mV) with a critical micellar concentration (CMC) of about 0.3 μg/ml. In contrast, the mean diameter of Pluronic F127 micelles was 27.1 (±3.2 nm) and the zeta potential was −0.30 mV (±0.17 mV), consistent with literature values (*24*, *25*).

PBC micelle–Ag engagement with BCRs

We investigated the underlying mechanism of B cell activation that leads to the observed in vivo responses in mice immunized with PBC micelle–Ag formulations. Our previous studies showed that the PBC micelles associated with Ag (*16*). Hence, to gauge the engagement of PBC micelle–Ag complexes with BCRs, analysis of endogenous Nur77 protein expression in B cells stimulated with PBC micelle–Ag was performed and compared with that induced by two controls: lipopolysaccharide (LPS; a TLR4 agonist) and anti–immunoglobulin M (IgM) F(ab′)$_2$. We also used Pluronic F127 micelles as a stimulant in our studies to better understand how the additional cationic blocks of the PBC micelles (whose parent molecule is Pluronic F127) help generate this type of B cell response. Nur77 is a well-studied specific marker for Ag receptor signaling for both B and T cells in mice and humans and reflects the strength of receptor signaling (*22*, *26*). We found that Nur77 was induced in murine splenic B cells (CD19$^+$) upon stimulation with PBC micelle–Ag complexes at levels similar to (control) stimulation (Fig. 1A). We also studied Nur77 induction at different time points of stimulation. Although at 2 hours after stimulation Nur77 induction for the PBC micelle–Ag treatment was not as pronounced as the anti-IgM F(ab′)$_2$ control, we observed robust induction at 4 hours after stimulation for both treatments, which declined to basal levels by 24 hours after stimulation. Similar kinetics have been previously reported for Nur77 induction (*22*). In contrast, LPS did not trigger Nur77 induction, consistent with the literature (Fig. 1B) (*22*). Cells stimulated with Pluronic F127 micelle–Ag were also evaluated and failed to effectively induce Nur77, indicating the nonengagement of BCRs with these micelles. These studies show that the cationic PBC micelles specifically engaged B cells via interactions with the BCR.

B cell activation via BCR cross-linking by PBC micelles

Together, the observations of short-term antibody responses generated by PBC micelles, nonactivation of APCs, and engagement of PBC micelle–Ag with BCRs all led us to investigate the mechanism of B cell activation by cross-linking of BCRs. To test our hypothesis, B cell proliferation from splenic cells isolated from wild-type (WT) C57BL/6 mice was investigated by using a carboxyfluorescein diacetate succinimidyl ester (CFSE) proliferation assay (*27*). The schematic of this study is shown in the top panel of Fig. 2A. To demonstrate BCR cross-linking, anti-IgM F(ab) fragments were used with or without PBC micelles to stimulate the splenic cells. Anti-IgM F(ab′)$_2$ (10 μg/ml) was used as a positive control. Anti-CD40 (5 μg/ml) was added to all treatment groups, except unstimulated medium-only control, to provide a costimulatory signal. After 5 days in culture, the viability of B cells (Zombie Aqua$^-$CD3$^-$CD19$^+$B220$^+$) was observed to be lower for the cells stimulated with F(ab) fragments alone (10 μg/ml), PBC micelle alone (10 μg/ml), and unstimulated controls (medium only) than for cells stimulated with either F(ab′)$_2$ (positive control) or

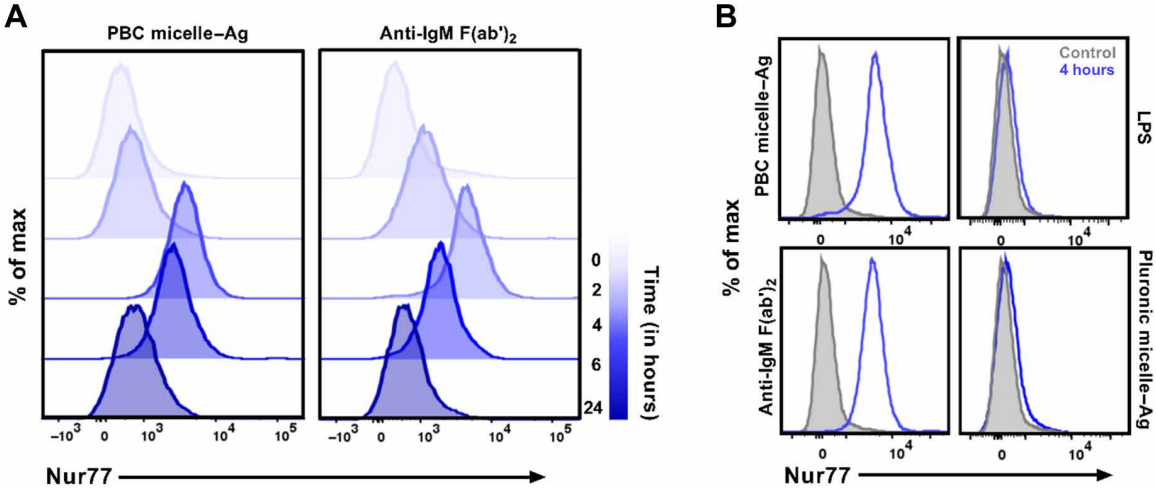

Fig. 1. Up-regulation of Nur77 by PBC micelle–Ag complexes. (**A**) Representative histograms for Nur77 antibody expression in B cells. Total splenic cells following RBC lysis from C57BL/6 mice stimulated with either PBC micelle–Ag or Pluronic F127 micelle–Ag (at 10 μg/ml each component) are shown. LPS (0.5 μg/ml) and anti-IgM Fa(ab′)$_2$ (10 μg/ml) were used as controls. Cells were stained for cell surface marker (CD19) for B cell gating and intracellularly stained for Nur77 antibody at 2, 4, 6, or 24 hours after stimulation. Cells analyzed at 0 hour after stimulation were shown to indicate background levels of Nur77 expression. (**B**) Representative histograms for Nur77 induction following 4 hours (peak) of stimulation for four treatment groups (blue lines) and unstimulated control (light gray, filled). Data are representative of three independent experiments.

Downloaded from http://advances.sciencemag.org/ on August 11, 2021

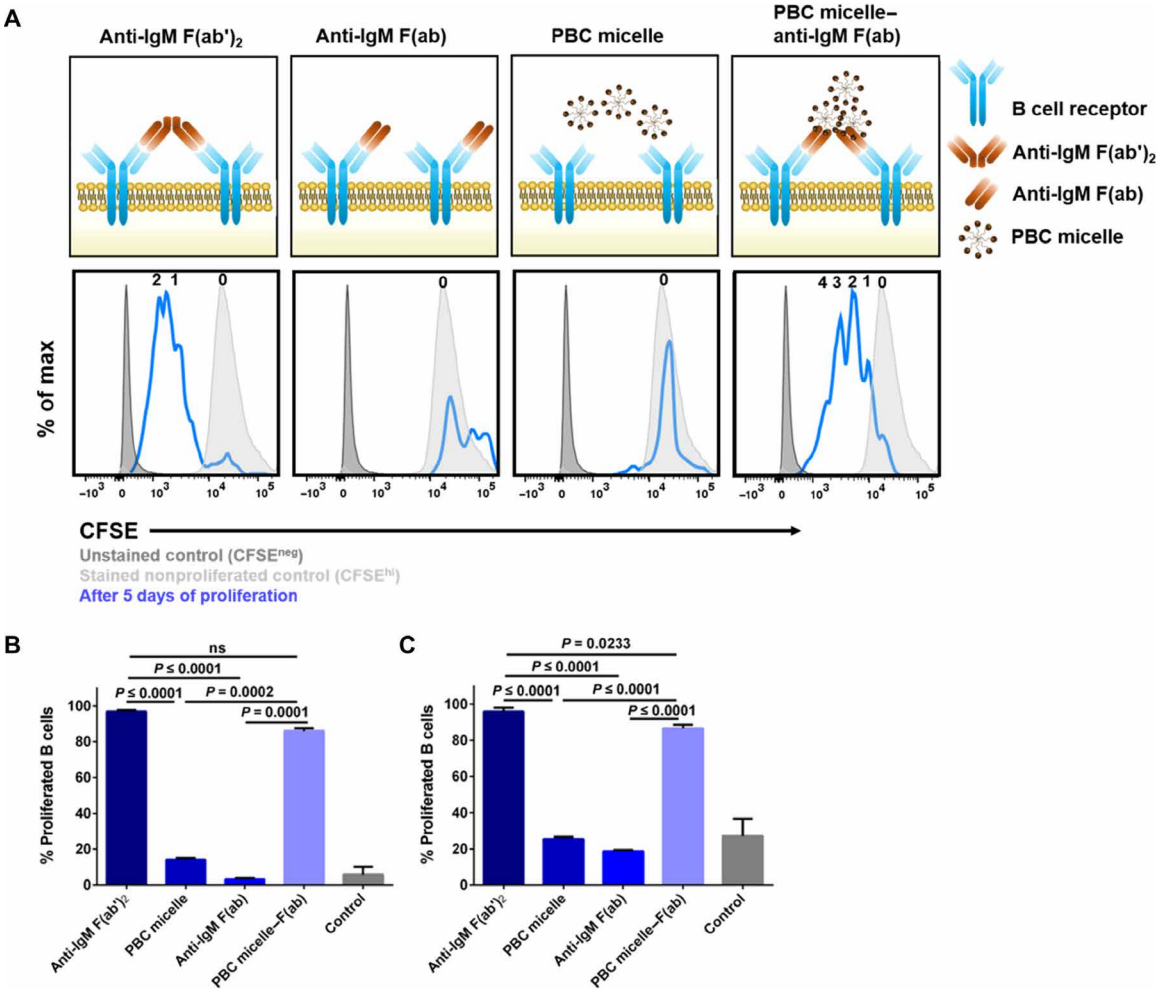

Fig. 2. PBC micelle–anti-IgM Fab complexes cross-link BCRs and induce B cell proliferation. (**A**) Top: Schematic of the experiment showing stimulation of WT murine spleen cells following RBC lysis with anti-IgM F(ab')$_2$ (10 μg/ml), anti-IgM F(ab) (10 μg/ml), PBC micelles (10 μg/ml), or PBC micelle–anti-IgM F(ab) (10 μg/ml each). Anti-CD40 (5 μg/ml) was added to all the treatment groups except unstimulated controls. Bottom: Corresponding representative histograms for the stimulation groups with CFSE expression for viable B cells (Zombie$^-$CD3$^-$CD19$^+$B220$^+$) from flow cytometry. The histograms (blue lines) were generated 5 days after proliferation. The number of daughter populations is indicated in a row on top of each histogram (i.e., zero = nonproliferating parent peak). Peaks for CFSE-unstained cells (dark gray, filled) and CFSE-stained nonproliferated cells (light gray, filled) are also shown. (**B**) Percent proliferated viable B cells from spleens as determined by CFSE^{lo} gating for young mice. ns, not significant. **C**) Percent proliferated viable B cells from spleens as determined by CFSE^{lo} gating for aged mice. For cell culture, splenic cells (0.5×10^6 cells per well) were stimulated in 96-well U-bottom plates. Data are represented as mean ± SEM. Data were analyzed using one-way analysis of variance (ANOVA) followed by Tukey's post hoc test; $n = 5$; ns, not significant. In addition to the significance denoted in the image with the respective P values, mean values for anti-F(ab')2 and PBC micelle–anti-IgM F(ab) are also statistically significant from control for (B) and (C) with $P < 0.0001$, and PBC micelle and anti-IgM F(ab) groups are not significant from control.

PBC micelle–F(ab), indicating that only these two treatments provided the required survival signal to B cells (fig. S2A).

Investigating the proliferation of B cells, multiple proliferation peaks (i.e., CFSE^{lo}) were detected corresponding to daughter populations for cells stimulated with either F(ab′)$_2$ or PBC micelle–F(ab) (Fig. 2A, bottom), in contrast to cells stimulated with F(ab) fragments alone or PBC micelle alone (which only show the CFSE^{hi} parent peak). It is also noteworthy that for PBC micelle–F(ab) stimulation, provision of anti-CD40 signal was not required for B cell activation and proliferation. However, we observed a relatively higher number of viable B cells when anti-CD40 was present (92.1% versus 79.8%; fig. S2B). The percentage of B cells that proliferated was found to be similar for F(ab′)$_2$ and PBC micelle–F(ab) at 80 to 90% (Fig. 2B). We also tested and observed the same effect with B cells isolated from spleens of aged (20- to 22-month-old) WT mice (Fig. 2C), further underlying the value of using PBC micelle–based adjuvants in enhancing B cell proliferation in aged immune systems.

Furthermore, we investigated BCR cross-linking–induced B cell proliferation for various concentrations of PBC micelle–F(ab) and observed B cell proliferation at PBC micelle concentrations as low as 1 μg/ml (fig. S2C). This effect was not observed for PBC unimers (at a concentration of 0.1 μg/ml—below the CMC for PBC micelles) or for Pluronic F127 micelles at 10 μg/ml (fig. S2D), indicating that polymer properties such as the PBC chemical structure, its cationic nature, and its micellar phase are necessary for this cross-linking.

Downloaded from http://advances.sciencemag.org/ on August 11, 2021

Ag-specific B cell proliferation induced by PBC micelle–Ag complexes

To investigate whether BCR cross-linking also occurs upon use of PBC micelle–Ag complexes, similar studies were performed where splenic cells from WT BALB/c and C57BL/6 mice were stimulated with Ag (10 μg/ml) with or without PBC micelles (10 μg/ml) (Fig. 3A). Both model Ag used for these studies [i.e., hen egg lysozyme (HEL) and ovalbumin (OVA)] showed similar results. A clear distinction was observed between the total number of viable B cells stimulated with Ag alone versus PBC micelle–Ag complexes (fig. S3A). In terms of B cell proliferation, a significantly higher percentage of proliferation with multiple daughter peaks ($CFSE^{lo}$) was observed after stimulation with PBC micelle–Ag complexes compared to Ag alone (Fig. 3, A and B). Next, we analyzed whether these proliferated B cells secreted Ag-specific antibodies. We measured anti-IgM titers in the supernatants of the cells 10 days after stimulation with different Ag with or without PBC micelles. We observed significantly higher levels of anti-HEL or anti-OVA titers when the cells were stimulated with the PBC micelles, in contrast to the respective Ag-only stimulation (Fig. 3, C and D). The supernatant samples from cells stimulated with all the Ag groups were analyzed for Ag-specific IgM. The titers for nonspecific antibodies induced by the PBC micelle–Ag complex were found to be negligible. We used anti-$F(ab')_2$ again as a positive control for stimulation of the cells and observed that this treatment induced significantly higher levels of B cell proliferation than that induced by the PBC micelle–Ag complexes. However, the Ag-specific antibody response data indicated that these B cells were producing a low level of nonspecific antibodies, similar to that of the medium-only

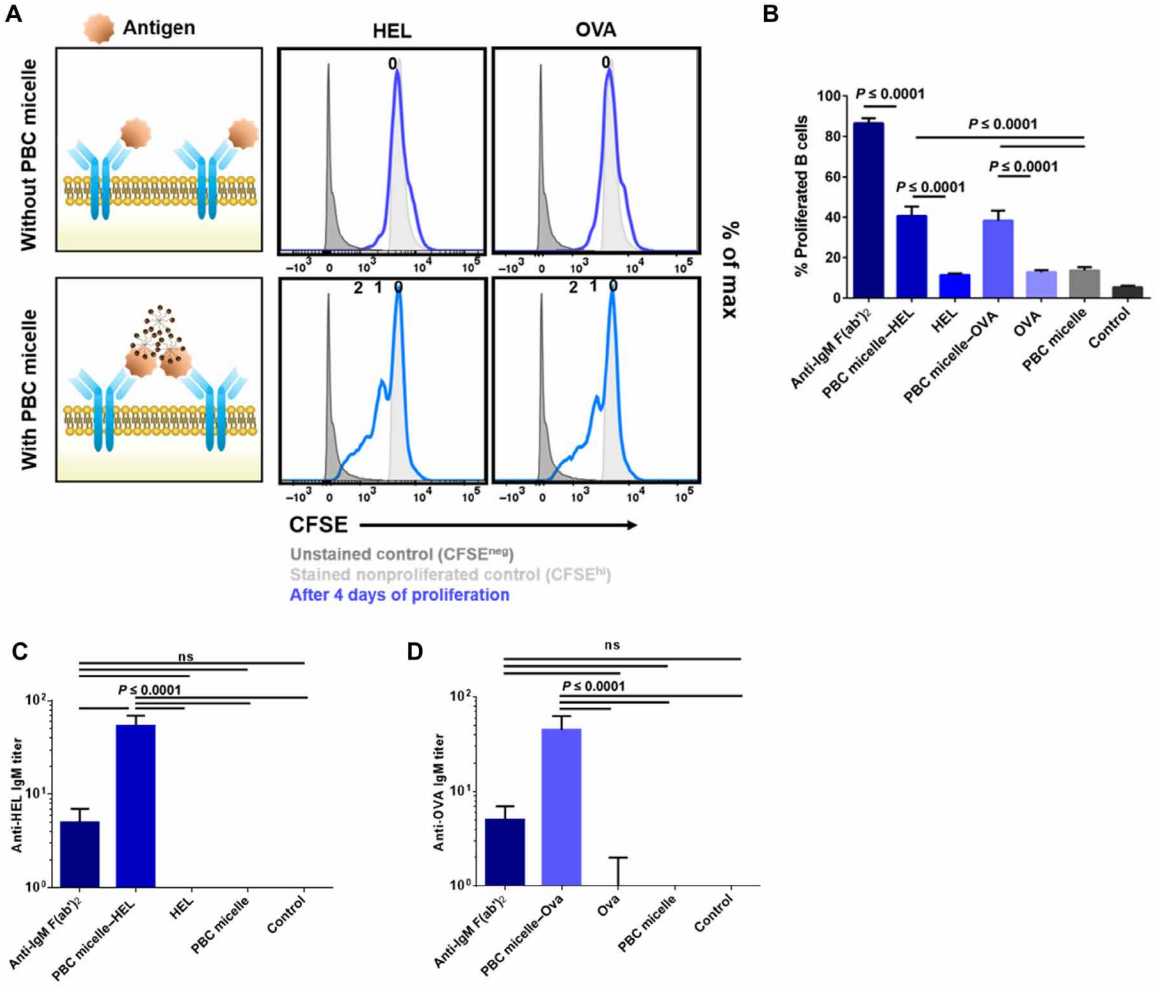

Fig. 3. PBC micelle–Ag complexes enhance B cell proliferation and antibody production. (**A**) Schematic of experiment showing stimulation of murine spleen cells following RBC lysis with the following treatment groups: anti-IgM $F(ab')_2$ (10 μg/ml) as positive control, Ag only [Ag: hen egg white lysozyme (HEL) or ovalbumin (OVA)], PBC micelles only (10 μg/ml), or PBC micelle–Ag (10 μg/ml each). Anti-CD40 (5 μg/ml) was added to all the treatment groups except unstimulated controls. Corresponding representative histograms for the stimulation groups with CFSE expression (blue lines) for viable B cells ($Zombie^-CD3^-CD19^+B220^+$) generated 4 days after proliferation. The number of daughter populations is indicated in a row on top of each histogram (i.e., zero = nonproliferating parent peak). Peaks for CFSE-unstained cells (light gray, filled) are also shown. (**B**) Percent proliferated viable B cells from spleens as determined by $CFSE^{lo}$ gating for young WT mice. (**C**) Anti-HEL IgM titers and (**D**) anti-OVA IgM titers in the supernatants of cells stimulated with different treatment groups. For cell culture, splenic cells (0.5×10^6 cells per well) were stimulated in 96 well U-bottom plates. Experiments were performed with cells from both C57BL/6 and BALB/c mice. Data are represented as mean ± SEM. Data were analyzed using one-way ANOVA followed by Tukey's post hoc test; $n = 4$. In addition to the significance denoted in the image with the respective P values, mean values for anti-F(ab')2 and PBC micelle–Ag groups in (B) are also statistically significant from control with $P < 0.0001$. PBC micelle, HEL, and OVA are not significant from the medium-only control in (B) to (D).

Downloaded from http://advances.sciencemag.org/ on August 11, 2021

control group. Similar to the PBC micelle–F(ab) stimulation, provision of anti-CD40 signal was not required for B cell activation and proliferation with PBC micelle–Ag complexes. However, the anti-CD40 signal was required for antibody production (fig. S3B). Again, no significant B cell proliferation was observed for cells stimulated with Ag in combination with either PBC unimers or Pluronic F127 micelles (fig. S3C). Together, these studies indicate that the PBC micelle–Ag complexes induced Ag-specific B cell proliferation, in contrast to PBC unimers or micelles of other synthetic chemistries.

PBC micelle scaffolds for Ag presentation to B cells

Next, we investigated the proliferation of B cells stimulated with PBC micelle–Ag complexes in a transgenic (Ighel Tg) mouse model (*28*), in which majority of BCRs on splenic B cells are specific to HEL. Our hypothesis was that the increase in Ag-specific BCR repertoire would lead to enhanced PBC micelle–Ag complex–BCR engagement and, hence, increased B cell proliferation (compared to WT mice). Splenic cells isolated from Ighel Tg mice were cultured and stained with CFSE, following which they were stimulated with HEL alone (10 μg/ml), PBC micelle (10 μg/ml) alone, or PBC micelle–HEL complexes. Given the increased number of HEL-specific BCRs in these mice as compared to WT mice, we observed a small peak with some proliferation in cells stimulated with the HEL-only group (Fig. 4A). Notably, at least five proliferation peaks ($CFSE^{lo}$) for the corresponding daughter populations were observed for the B cells stimulated with the PBC micelle–HEL complex. The viable B cell population 4 days after stimulation was also the highest for this group (fig. S4A). The percentage of proliferated B cells was twice as high with the Ighel Tg mouse model (about 80%), in contrast to WT mice (about 40%) as shown in Figs. 3B and 4B, supporting our hypothesis. We measured anti-HEL IgM in the supernatants and found significantly higher levels of antibody secretion from cells stimulated with the PBC micelle–HEL complex, compared to HEL alone (Fig. 4C). The anti-HEL IgM titers in supernatants of cells stimulated with PBC micelle–HEL complex for the Ighel Tg mice were about 2.5-fold higher than that measured in cell supernatants from WT mice, correlating with the higher proliferation (Figs. 3, B and C, and 4, B and C). In contrast, stimulation with Pluronic F127 micelles + HEL or PBC unimers + HEL did not lead to B cell proliferation (fig. S4C), once again confirming that just the PBC micelle–Ag complex induced Ag-specific B cell proliferation. These observations suggest that the PBC micelles must be acting as a scaffold for Ag that is able to stimulate B cells and lead to the generation of Ag-specific antibodies.

PBC micelle platform for in vitro antibody production

Because we observed anti-IgM antibodies in the supernatants of the B cells stimulated with the PBC micelle–Ag complexes for the model Ag, we sought to determine whether these observations could be exploited by using these scaffolds as a platform technology for the production of therapeutic antibodies in vitro. To investigate this, we used S protein from SARS-CoV-2 and recombinant fusion protein F1-V from *Y. pestis* with the PBC micelles and evaluated in vitro production of antibodies and B cell proliferation using CFSE as described previously. Our results were consistent with the experiments with the model Ag and indicated that cells stimulated with the PBC micelle–Ag complexes exhibited daughter cell populations, but cells stimulated with Ag only or with Pluronic F127 micelle + Ag or PBC unimers + Ag did not (Fig. 5, A, B, D, and E). As a result, only cell culture supernatants in cells stimulated with the PBC micelle–Ag complexes showed anti-S IgM or anti–F1-V IgM (Fig. 5, C and F). Although we observed proliferation in the cells stimulated with anti-IgM $F(ab)_2$ (positive control), we did not observe Ag-specific antibodies in the supernatants of these cells. Hence, the ability of the PBC micelle scaffolds to cross-link BCRs, combined with the synergistic effect provided by costimulatory signals induced by anti-CD40, could be exploited as a novel platform technology for rapid and efficient production of Ag-specific therapeutic antibodies, which may be effective in the treatment of individuals affected by diseases such as COVID-19 or pneumonic plague.

DISCUSSION

Host immune responses generated following vaccination can be complex and diverse in nature, with B cell responses being an essential contributor toward conferring protective immunity (e.g., antibody-mediated viral and toxin neutralization). Hence, the design of vaccine adjuvants has largely been focused on improving B cell and antibody responses (*29*).

An in-depth understanding of the mechanisms of B cell activation by different types of adjuvants that drive the induction of protective antibody responses has been extensively explored (*30*, *31*). It

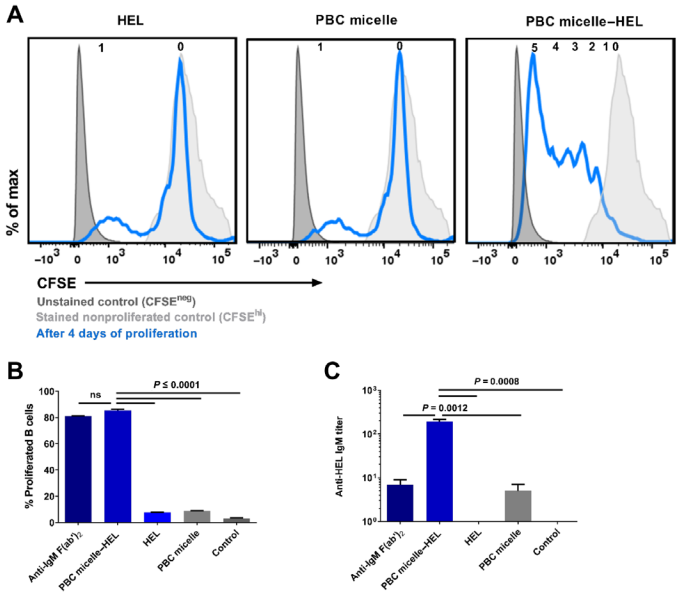

Fig. 4. Ag presentation to B cells by PBC micelles in Tg mice. (**A**) Representative histograms for CFSE-stained (blue lines) viable B cells ($Zombie^{-}CD3^{-}CD19^{+}B220^{+}$) 4 days after stimulation of splenic cells from C57BL/6-Tg(IghelMD4)4Ccg/J mice with various treatment groups [anti-IgM $F(ab')_2$, HEL, and PBC micelles at 10 μg/ml]. Anti-CD40 (5 μg/ml) was added to all the treatment groups except unstimulated controls. The number of daughter populations is indicated in a row on top of each histogram. Peaks for CFSE-unstained cells (dark gray, filled) and CFSE-stained nonproliferated cells (light gray, filled) are also shown. (**B**) Percent proliferated viable B cells as determined by $CFSE^{lo}$ gating. (**C**) Anti-HEL IgM in the supernatants of cells stimulated with different treatment groups for 10 days. For cell culture, splenic cells (0.5×10^6 cells per well) were stimulated in 96-well U-bottom plates. Data are represented as mean ± SEM. Data were analyzed using one-way ANOVA followed by Tukey's post hoc test; $n = 4$ animals per group. In addition to the significance denoted in the image with the respective P values, mean values for PBC micelle and HEL are not significant from medium-only control in (B) and (C).

Downloaded from http://advances.sciencemag.org/ on August 11, 2021

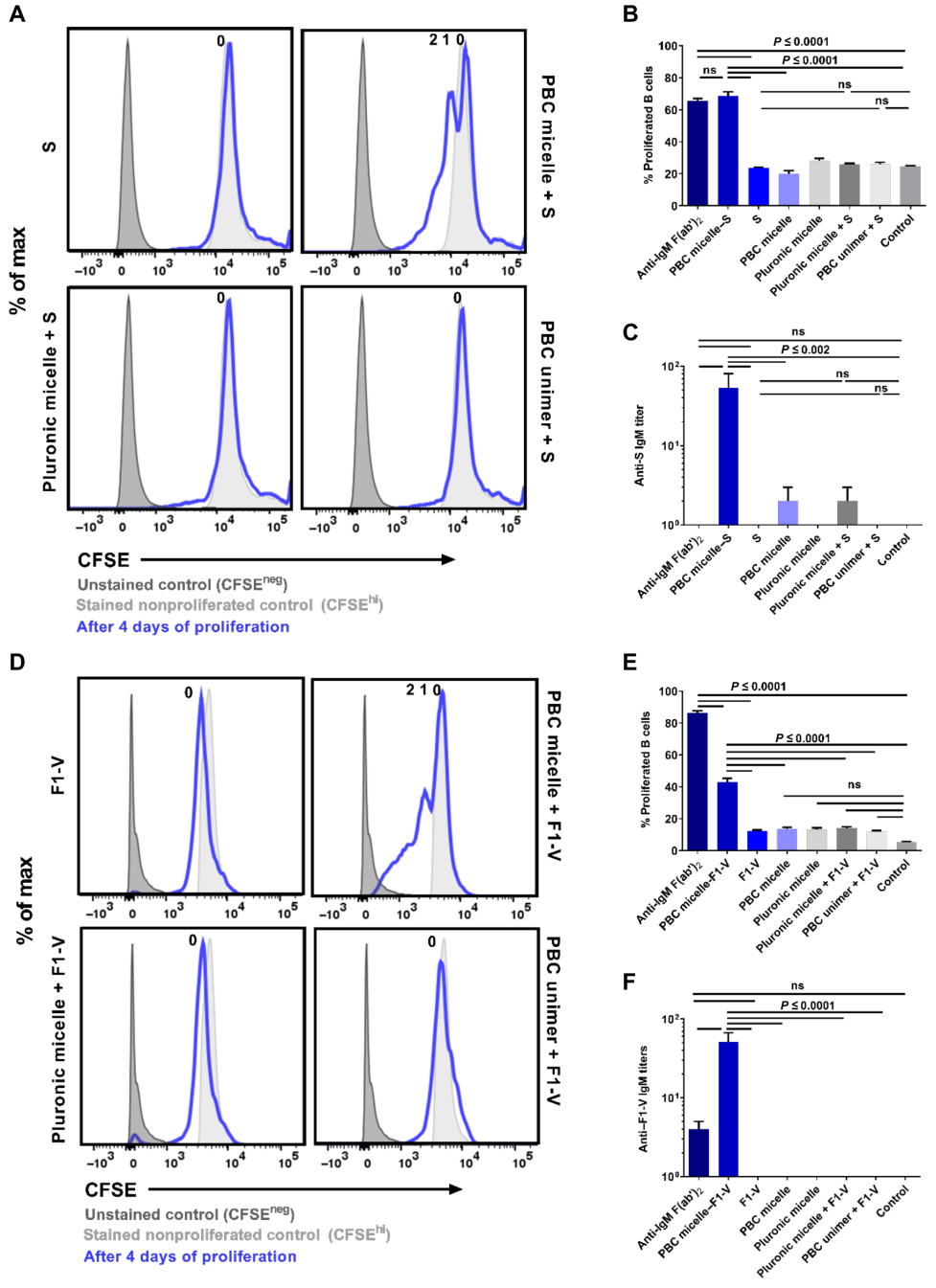

Fig. 5. PBC micelles serve as a platform for in vitro therapeutic antibody production. Splenic cell population obtained from WT C57BL/6 mice or BALB/c mice following RBC lysis was stimulated in 96-well U-bottom plates at a density of 0.5×10^6 per well. Anti-CD40 (5 μg/ml) was added to all the treatment groups except unstimulated controls. S protein from SARS-CoV-2 (10 μg/ml) and F1-V from *Y. pestis* (10 μg/ml) was used with or without PBC micelles (10 μg/ml), Pluronic F127 micelles (10 μg/ml), or PBC unimers (10 μg/ml). (**A**) Histograms depicting CFSE levels of B cells stimulated with various treatment groups with or without S protein for 4 days. (**B**) Percent proliferated viable B cells as determined by $CFSE^{lo}$ gating. (**C**) Anti-S IgM titers measured in the supernatants of the stimulated cells after 10 days. (**D**) Histograms depicting CFSE levels of B cells stimulated with various treatment groups with or without F1-V for 4 days. (**E**) Corresponding percent proliferated viable B cells as determined by $CFSE^{lo}$ gating. (**F**) Anti–F1-V IgM titers measured in the supernatants of the stimulated cells after 10 days. Data are represented as mean ± SEM. Data were analyzed using one-way ANOVA followed by Tukey's post hoc test; $n = 2$ to 4. PBC micelle, S protein, F1-V, Pluronic F127 micelle, and PBC unimers are not significant from medium-only control.

is well known that traditional adjuvants have multiple functions, including APC activation, enhanced cytokine secretion, and serving as Ag depots. However, the mechanism(s) underlying B cell activation by synthetic polymer micelle–based adjuvants is relatively unknown. In this work, we studied the mechanism of activation of cationic PBC micelle adjuvants. While pursuing this, we made the novel discovery that the same mechanism(s) may not be operative for all types of micellar adjuvants, calling for the use of appropriate

Downloaded from http://advances.sciencemag.org/ on August 11, 2021

adjuvant chemistries for specific applications instead of a "one-size-fits-all" approach.

It is well known that, unlike T cells, B cells can recognize Ag in its native form and that the activation of B cells can be mediated in a T cell–independent manner (*32*). This process involves the cross-linking of the BCRs by repetitive or complexed/aggregated Ag, which would up-regulate Nur77 expression. Our studies demonstrated that PBC micelles, shown previously to associate with Ag (*16*, *33*), can facilitate cross-linking of BCRs, resulting in B cell activation. We first investigated the interaction of the PBC micelle–Ag complexes with the BCRs by analyzing Nur77 expression. Nur77/NR4A1 belongs to a subfamily of orphan nuclear receptors known as NR4A (encoded in the *Nr4a1-3* gene) (*26*), which plays an important role in cell survival and inflammatory signaling events. Nur77 expression has also been shown to be rapidly induced following BCR engagement by Ag, resulting in intracellular signaling (*34*). The engagement of BCRs with PBC micelle–Ag complexes led to the induction of a strong BCR signal that was similar to that induced by anti-IgM $F(ab')_2$ (Fig. 1). In contrast, other synthetic micelle chemistries such as the nonionic Pluronic F127 or the nonmicellar PBC unimers did not induce Nur77 expression. These results support our hypothesis that the biomaterial chemistry, its cationic nature, and the ability to form micelles all play a crucial role in enhancing interactions between Ag and BCRs. In addition, it is likely that the PBC micelles are activating T cells because we previously demonstrated that the PBC micelles efficiently deliver Ag to the cytosols of dendritic cells (*16*).

To demonstrate BCR cross-linking by the PBC micelles, we used anti-IgM $F(ab')_2$ and anti-IgM F(ab) fragments. The first report of the cross-linking model of B cell activation also used these molecules and showed that while monomeric anti-IgM F(ab) fragments bind to but do not activate B cells, dimeric anti-IgM $F(ab')_2$ fragments do (*35*). Our results (Fig. 2) were consistent with these observations and, in addition, showed that when the monomeric anti-IgM F(ab) fragments were combined with PBC micelles, B cell survival and proliferation were induced (Fig. 2). It was notable that this enhanced B cell proliferation was also observed in aged animals (Fig. 2C), underlying the value of using PBC micelle–based adjuvants in vaccines for aged immune systems. As mentioned previously, including adjuvants in vaccine formulations that can enhance immune responses without exacerbating chronic inflammation in aged individuals may lead to beneficial immune responses (*19*–*21*).

We also demonstrated that PBC micelle–Ag complexes induced a higher degree of B cell activation and proliferation compared to soluble Ag alone or Ag associated with PBC unimers or micelles of other chemistries, owing to BCR cross-linking by the PBC micelle–Ag complexes (Fig. 3 and fig. S3). Antigenic epitope density has been previously linked to Ag recognition and the efficiency of B cell responses, especially for T-independent Ag with repeating epitopes (*36*). There have also been reports of engineered synthetic particles that can exhibit repetitive orientation of antigenic epitopes (*37*). The PBC micelles, by virtue of their association with Ag, may be providing a scaffold-like structure that orients Ag as high epitope density complexes that facilitate cross-linking of BCRs. In addition, the use of vaccine adjuvants that create a similar multivalent display of Ag has been shown to lead to a balanced T helper 1 (T_H1)/T_H2 response (*38*). This type of balanced response is vital for clearing viral infections, in which both neutralizing antibody and cytotoxic T cells are important to induce protective immunity (*39*).

It is noteworthy that the presence of anti-CD40 was not required for inducing B cell proliferation. However, we observed a higher degree of proliferation with anti-CD40, and its addition was a requirement for the production of antibodies (figs. S2B, S3B, and S4B). This is consistent with reports in the literature showing that the engagement of both the BCR and CD40 leads to a synergistic activation of B cells through distinct cellular pathways and that a costimulatory signal is required for inducing B cell differentiation (*40*, *41*). According to another report, while maximal B cell proliferation could be achieved without anti-CD40 signal (T cell help), the B cells failed to differentiate into antibody-producing cells (i.e., plasma cells) (*42*).

In addition to increasing the valency of Ag by using PBC micelles, we showed that the recognition of PBC micelle–Ag complexes by BCRs is also proportional to the number of Ag-specific BCRs using a Tg mouse model with splenic cells consisting of HEL-specific BCRs. Greater B cell proliferation was accompanied by higher antibody secretions from B cells of Ighel Tg mice compared to WT mice (Figs. 3, B and C, and 4). We hypothesize that the PBC micelles act as a scaffold to orient Ag for efficient presentation and cross-linking of the BCRs, resulting in activation and terminal differentiation into antibody-secreting plasma cells. These observations are consistent with the spatial orientation of BCRs and the need to effectively cluster BCRs by taking advantage of the scaffolding capabilities of the PBC micelle (*43*). A similar concept for using synthetic materials to act as scaffolds for vaccine delivery has been reported previously, and our PBC micelles and the experiments herein provide support to this concept (*44*). Furthermore, the enhanced responses induced by the PBC micelles mixed with HEL likely indicate that this complex may lower the mechanical force threshold required to initiate BCR clustering (*43*, *45*). The desired outcome of Ag–B cell interactions would be to induce germinal center formation, memory B cells, and long-lived plasma cells (*46*). Given that the affinity of Ag for BCRs governs the activation and differentiation of naive B cells, we hypothesize that the use of the PBC micelles effectively increases the affinity of the Ag-BCR interaction by (i) extending the dwell time that Ag and BCRs interact, (ii) allowing the generation of larger BCR clusters, and (iii) inducing B cell proliferation and differentiation resulting in a more robust B cell response than induced by Ag alone (*43*, *46*).

Our studies showed that BCR cross-linking is Ag dependent and is not induced by using either polymeric chains that have not formed micelles (i.e., PBC unimers below the CMC) or other self-assembled synthetic micelle-based formulations (such as nonionic Pluronic F127) (figs. S2D, S3C, and S4C). As the Pluronic F127 triblock copolymer is a part of the PBC and forms micelles of the same size, it serves as an inherent control for comparison. It appears that the outer cationic PDEAEM blocks in the PBC micelles, which are not present in Pluronic F127, are playing a major role toward interacting with and presenting Ag, thus enabling the observed BCR cross-linking.

We also demonstrated that this type of B cell activation by PBC micelles can prove to be beneficial in the context of providing an efficient and fast method for the production of therapeutic antibodies in vitro. Antibodies are being used extensively as therapeutics for the treatment of several diseases and can prove to be effective therapies for new and emerging diseases (*47*, *48*). This has been exemplified during the COVID-19 pandemic with emergency use approval from the FDA of multiple antibody therapies to treat individuals with SARS-CoV-2 infections, which has reduced hospitalizations and deaths (*49*). We exploited the B cell activation mechanisms of

Downloaded from http://advances.sciencemag.org/ on August 11, 2021

PBC micelles to demonstrate production of Ag-specific antibodies that bind to multiple pathogenic Ag (i.e., S protein from SARS-CoV-2 and F1-V from *Y. pestis*) in the supernatants of the cells stimulated with PBC micelle–Ag complexes (Fig. 5), indicating the versatility and further added value of this approach as a platform technology.

The enhancement in the in vivo antibody response induced by the PBC micelles was short-lived, in contrast to that induced by a traditional adjuvant such as monophosphoryl lipid A (MPLA) (fig. S5). However, immunization with a combination of PBC micelles and MPLA induced a synergistic enhancement in the antibody response due to BCR cross-linking by the PBC micelles and immunoglobulin isotype switching facilitated by MPLA (figs. S5 and S6) (*50*). These results provide strong rationale for the use of combination adjuvants that may be beneficial in scenarios where both antibody isotypes and the induction of both rapid and long-lived immunity are important components of protective immunity. Our previous work has shown the value of such a combination adjuvant strategy in the design of nanovaccines against pneumonic plague and influenza A virus (*51*–*53*).

In summary, the PBC micelles provide a promising platform not only for rational design of vaccine adjuvants but also for the production of therapeutic antibodies. For many vaccine formulations, a combination of adjuvants is required for generating an optimal immune response, which calls for a better understanding of the mechanism of action of these adjuvants. This work, which is focused on understanding the mechanism of action of PBC micelle adjuvants, is an important step closer toward that goal. Our studies implicate BCR cross-linking as a possible mechanism of action for PBC micelle adjuvants in B cell activation. Last, the production of therapeutic antibodies in vitro with this platform has the potential to be a disruptive technology for rapid availability of such countermeasures, especially in the face of a global pandemic. All these attributes position the PBC micelle platform as a highly versatile tool in the development of multiple countermeasures against emerging and reemerging infectious diseases.

MATERIALS AND METHODS

Materials

N,*N*-(diethylamino)ethyl methacrylate (DEAEM), Pluronic F127, HEL, IgG from rat serum, and Triton X-100 were purchased from Sigma-Aldrich (St. Louis, MO). Goat anti-mouse IgM F(ab′)$_2$ fragment, goat anti-mouse IgM Fab fragment, and alkaline phosphatase–conjugated anti-mouse IgM were purchased from Jackson ImmunoResearch Laboratories Inc. (West Grove, PA). Endotoxin-free OVA was purchased from InvivoGen (San Diego, CA). *Y. pestis* fusion protein F1-V (NR-4526) was obtained from the Biodefense and Emerging Infections Repository (Manassas). SARS-CoV-2 S protein was purchased from GenScript (Piscataway, NJ). Antibodies for flow cytometry [phycoerythrin (PE) anti-mouse CD19, allophycocyanin/Cyanine 7 (Cy7) anti-mouse B220, Zombie Aqua viability kit, PE-Cy7 anti-mouse Nur77, and peridinin chlorophyll protein (PerCp)–Cy5.5 anti-mouse CD3 and anti-CD16/32] and purified anti-mouse CD40 antibody were purchased from BioLegend (San Diego, CA). BD stabilizing fixative was purchased from BD Biosciences (Franklin Lakes, NJ). All other chemicals and materials were purchased from Fisher Scientific (Pittsburgh, PA).

PBC synthesis and characterization

PBC was synthesized by atom transfer radical polymerization as previously reported (*23*). This involves the formation of a difunctional macroinitiator from Pluronic F127 as the first step. Next, the macroinitiator and the monomer, DEAEM, were reacted using copper (I) oxide nanoparticles as the catalyst and *N*-propylpyrilidinemethanamine (NPPM) as the complexing ligand. The molecular weight of the resulting PBC was determined using ^{1}H NMR. For the micelle formulation, a stock solution of 50 mg/ml total polymer concentration (either PBC or Pluronic F127) was prepared in phosphate-buffered saline (PBS). The stock solution was diluted to the required concentrations and mixed with the Ag before stimulation of cells. For characterizing the size, zeta potential, and CMC of PBC and Pluronic F127 micelles, dynamic light scattering measurements with Zetasizer Nano S (Malvern PANalytical, Westborough, MA) were carried out.

Animals

Female BALB/c and C57BL/6 mice (6 to 8 weeks old or 20 to 22 months old) and C57BL/6-Tg(IghelMD4)4Ccg/J mice (6 weeks old) were purchased from The Jackson Laboratory (Bar Harbor, ME). The Institutional Animal Care and Use Committee at Iowa State University approved all the protocols involving animals.

Immunization and serum collection

To evaluate antibody responses, C57BL/6 mice were subcutaneously immunized with 100 μl of the PBC micelle (5 mg per dose) formulation or MPLA (10 μg per dose) formulation or MPLA and PBC micelle formulation with 50 μg of either HEL or OVA Ag. Control animals were immunized with soluble HEL or OVA in PBS (50 μg in 100 μl) (i.e., no adjuvant). Serum samples were collected via the saphenous vein at 2, 4, 6, 8, and 10 weeks after immunization.

Tissue isolation and cell culture

Following euthanasia, the spleens of mice (BALB/c and C57BL/6) were excised, and a single-cell suspension was prepared using a handheld tissue homogenizer. The tissue culture medium consisted of RPMI 1640, penicillin (100 U/ml), streptomycin (100 μg/ml), and 10% fetal bovine serum. Red blood cell (RBC) lysis was performed to remove erythrocytes from the cell suspension, and the resulting splenocytes were washed with medium before counting the cells. One set of splenocytes was labeled with CFSE for analyzing cell proliferation after stimulation. The cells were stained with CFSE on day 0 after isolation from spleens using standard procedure. Micelles and Ag were mixed thoroughly by pipetting up and down and co-incubated at the required combination of concentrations for 30 min at room temperature. The CFSE-labeled cells were stimulated with different treatment groups for 4 to 5 days. After stimulation, cells were stained with antibodies for flow cytometry.

The other set of splenocytes was directly used for stimulation and collection of supernatants 10 days after stimulation. For the plating, the splenocytes (with or without CFSE stains) were plated in 96-well U-bottom tissue culture plates at a cell density of 5×10^5 cells per well with 200 μl of medium in each well. The cells were stimulated with different combinations of treatment groups and concentrations. Similar cell density and stimulant concentrations were used for the Nur77 expression studies in 96-well U-bottom tissue culture plates for various time periods of stimulation as indicated in Fig. 1.

Flow cytometry

B cell proliferation was detected using in vitro labeling of cells with CFSE and analysis by flow cytometry. Distinct generations of proliferating cells can be monitored by dilutions of CFSE stain on the

Downloaded from http://advances.sciencemag.org/ on August 11, 2021

cells as viewed on the flow cytometry plots. For the flow cytometry procedure, the cells were transferred into polystyrene fluorescence-activated cell sorting (FACS) tubes and labeled with Zombie Aqua dye for tracking viable cells after stimulation using the manufacturer's instructions. Next, Fc receptors on the cells were blocked using rat IgG (100 μg/ml) and anti-CD16/32 (10 μg/ml) and stained with specific antibodies for surface markers (CD19, CD3, and B220) to detect the B cells in the splenocytes. Following surface staining, cells were washed with PBS and then fixed with 4% *p*-formaldehyde. After washing the cells again with PBS, 0.1% Triton X-100 was used for permeabilization, and following that, anti-Nur77 antibody at a 1:50 dilution was used to intracellularly stain the cells. After all staining, cells were washed in FACS buffer to remove excess dye, and samples were fixed before analysis. Flow cytometry data were collected on FACSCanto II (BD Biosciences, Franklin Lakes, NJ) and analyzed using FlowJo (FlowJo LLC, Ashland, CA).

Antibody responses

Antibody levels in the sera collected from immunized animals at various time points (2, 4, 6, 8, and 10 weeks after immunization) and in the cell-free supernatants after 10 days of in vitro stimulation with various treatment groups were measured using enzyme-linked immunosorbent assay. Briefly, high-binding 96-well plates were coated with Ag (HEL, OVA, F1-V, or S protein) and blocked with 2% (w/v) of gelatin in 0.05% Tween-PBS solution. Sera samples were added to the plates starting at 1:200 dilution and then diluted 1:2 across the plate. Culture supernatant samples were added to the plates at a starting dilution of 1:3 and then diluted 1:3 across the plate. Alkaline phosphatase–conjugated anti-mouse IgG (H+L), IgG1, and IgG2c (Jackson ImmunoResearch, West Grove, PA) were used as the secondary antibody. The optical density was recorded at 405 nm using a SpectraMax M3 plate reader (Molecular Devices, San Jose, CA) after adding the substrate, and the titer was recorded as the last dilution that exhibited an optical density value that was twofold or higher than the background optical density.

Statistical analysis

All the data were analyzed using GraphPad Prism 8 software for statistical significance. For all figures, one-way analysis of variance (ANOVA) was used, followed by Tukey's post hoc test for multiple comparisons. For fig. S5, Kruskal-Wallis and Mann-Whitney tests were used to determine statistical significance.

SUPPLEMENTARY MATERIALS

Supplementary material for this article is available at http://advances.sciencemag.org/cgi/content/full/7/32/eabj1691/DC1

View/request a protocol for this paper from *Bio-protocol*.

REFERENCES AND NOTES

1. A. L. Mueller, M. S. McNamara, D. A. Sinclair, Why does COVID-19 disproportionately affect older people? *Aging* **12**, 9959–9981 (2020).
2. M. T. Ventura, M. Casciaro, S. Gangemi, R. Buquicchio, Immunosenescence in aging: Between immune cells depletion and cytokines up-regulation. *Clin. Mol. Allergy* **15**, 21 (2017).
3. R. L. Coffman, A. Sher, R. A. Seder, Vaccine adjuvants: Putting innate immunity to work. *Immunity* **33**, 492–503 (2010).
4. Y. Zhang, J. Xu, R. Jia, C. Yi, W. Gu, P. Liu, X. Dong, H. Zhou, B. Shang, S. Cheng, X. Sun, J. Ye, X. Li, J. Zhang, Z. Ling, L. Ma, B. Wu, M. Zeng, W. Zhou, B. Sun, Protective humoral immunity in SARS-CoV-2 infected pediatric patients. *Cell. Mol. Immunol.* **17**, 768–770 (2020).
5. P. J. Maglione, J. Chan, How B cells shape the immune response against Mycobacterium tuberculosis. *Eur. J. Immunol.* **39**, 676–686 (2009).
6. J. H. Lam, N. Baumgarth, The multifaceted B cell response to influenza virus. *J. Immunol.* **202**, 351–359 (2019).
7. T. Trimaille, B. Verrier, Micelle-based adjuvants for subunit vaccine delivery. *Vaccine* **3**, 803–813 (2015).
8. Z. Luo, Q. Wu, C. Yang, H. Wang, T. He, Y. Wang, Z. Wang, H. Chen, X. Li, C. Gong, Z. Yang, A powerful $CD8^+$ T-Cell stimulating D-tetra-peptide hydrogel as a very promising vaccine adjuvant. *Adv. Mater.* **29**, 1601776 (2017).
9. J. T. Wilson, S. Keller, M. J. Manganiello, C. Cheng, C. C. Lee, C. Opara, A. Convertine, P. S. Stayton, PH-responsive nanoparticle vaccines for dual-delivery of antigens and immunostimulatory oligonucleotides. *ACS Nano* **7**, 3912–3925 (2013).
10. S. Keller, J. T. Wilson, G. I. Patilea, H. B. Kern, A. J. Convertine, P. S. Stayton, Neutral polymer micelle carriers with pH-responsive, endosome-releasing activity modulate antigen trafficking to enhance $CD8^+$ T cell responses. *J. Control. Release* **191**, 24–33 (2014).
11. M. A. Julie Westerink, S. Louise Smithson, N. Srivastava, J. Blonder, C. Coeshott, G. J. Rosenthal, ProJuvant™ (Pluronic F127®/chitosan) enhances the immune response to intranasally administered tetanus toxoid. *Vaccine* **20**, 711–723 (2001).
12. C. Li, X. Zhang, Q. Chen, J. Zhang, W. Li, H. Hu, X. Zhao, M. Qiao, D. Chen, Synthetic polymeric mixed micelles targeting lymph nodes trigger enhanced cellular and humoral immune responses. *ACS Appl. Mater. Interfaces* **10**, 2874–2889 (2018).
13. A. K. Jain, A. K. Goyal, P. N. Gupta, K. Khatri, N. Mishra, A. Mehta, S. Mangal, S. P. Vyas, Synthesis, characterization and evaluation of novel triblock copolymer based nanoparticles for vaccine delivery against hepatitis B. *J. Control. Release* **136**, 161–169 (2009).
14. E. V. Batrakova, A. V. Kabanov, Pluronic block copolymers: Evolution of drug delivery concept from inert nanocarriers to biological response modifiers. *J. Control. Release* **130**, 98–106 (2008).
15. M. D. Determan, J. P. Cox, S. Seifert, P. Thiyagarajan, S. K. Mallapragada, Synthesis and characterization of temperature and pH-responsive pentablock copolymers. *Polymer* **46**, 6933–6946 (2005).
16. S. Senapati, R. J. Darling, D. Loh, I. C. Schneider, M. J. Wannemuehler, B. Narasimhan, S. K. Mallapragada, Pentablock copolymer micelle nanoadjuvants enhance cytosolic delivery of antigen and improve vaccine efficacy while inducing low inflammation. *ACS Biomater Sci. Eng.* **5**, 1332–1342 (2019).
17. R. J. Darling, S. Senapati, S. M. Kelly, M. L. Kohut, B. Narasimhan, M. J. Wannemuehler, STING pathway stimulation results in a differentially activated innate immune phenotype associated with low nitric oxide and enhanced antibody titers in young and aged mice. *Vaccine* **37**, 2721–2730 (2019).
18. C. A. Chougnet, R. I. Thacker, H. M. Shehata, C. M. Hennies, M. A. Lehn, C. S. Lages, E. M. Janssen, Loss of phagocytic and antigen cross-presenting capacity in aging dendritic cells is associated with mitochondrial dysfunction. *J. Immunol.* **195**, 2624–2632 (2015).
19. P. Marrack, A. S. McKee, M. W. Munks, Towards an understanding of the adjuvant action of aluminium. *Nat. Rev. Immunol.* **9**, 287–293 (2009).
20. J. U. McDonald, Z. Zhong, H. T. Groves, J. S. Tregoning, Inflammatory responses to influenza vaccination at the extremes of age. *Immunology* **151**, 451–463 (2017).
21. M. S. Abdul-Cader, A. Amarasinghe, M. F. Abdul-Careem, Activation of toll-like receptor signaling pathways leading to nitric oxide-mediated antiviral responses. *Arch. Virol.* **161**, 2075–2086 (2016).
22. J. F. Ashouri, A. Weiss, Endogenous Nur77 is a specific indicator of antigen receptor signaling in human T and B cells. *J. Immunol.* **198**, 657–668 (2017).
23. J. R. Adams, S. K. Mallapragada, Novel atom transfer radical polymerization method to yield copper-free block copolymeric biomaterials. *Macromol. Chem. Phys.* **214**, 1321–1325 (2013).
24. M. S. Aw, K. Gulati, D. Losic, Controlling drug release from Titania nanotube arrays using polymer nanocarriers and biopolymer coating. *J. Biomater. Nanobiotechnol.* **02**, 477–484 (2011).
25. J. Cacaccio, F. Durrani, R. R. Cheruku, B. Borah, M. Ethirajan, W. Tabaczynski, P. Pera, J. R. Missert, R. K. Pandey, F-127: An efficient delivery vehicle 3-(1′-hexyloxy)ethyl-3-devinylpyropheophorbide-a (HPPH or Photochlor). *Photochem. Photobiol.* **96**, 625–635 (2020).
26. C. Tan, J. L. Mueller, M. Noviski, J. Huizar, D. Lau, A. Dubinin, A. Molofsky, P. C. Wilson, J. Zikherman, Nur77 links chronic antigen stimulation to B cell tolerance by restricting the survival of self-reactive B cells in the periphery. *J. Immunol.* **202**, 2907–2923 (2019).
27. B. G. Hale, R. A. Albrecht, A. García-Sastre, Innate immune evasion strategies of influenza viruses. *Future Microbiol.* **5**, 23–41 (2010).
28. D. Y. Mason, M. Jones, C. C. Goodnow, Development and follicular localization of tolerant B lymphocytes in lysozyme/anti-lysozyme IgM/IgD transgenic mice. *Int. Immunol.* **4**, 163–175 (1992).

Downloaded from http://advances.sciencemag.org/ on August 11, 2021

29. K. Loré, G. B. Karlsson Hedestam, Novel adjuvants for B cell immune responses. *Curr. Opin. HIV AIDS* **4**, 441–446 (2009).
30. J. H. Wilson-Welder, M. P. Torres, M. J. Kipper, S. K. Mallapragada, M. J. Wannemuehler, B. Narasimhan, Vaccine adjuvants: Current challenges and future approaches. *J. Pharm. Sci.* **98**, 1278–1316 (2009).
31. E. A. Grego, A. C. Siddoway, M. Uz, L. Liu, J. C. Christiansen, K. A. Ross, S. M. Kelly, S. K. Mallapragada, M. J. Wannemuehler, B. Narasimhan, Polymeric nanoparticle-based vaccine adjuvants and delivery vehicles, in *Current Topics in Microbiology and Immunology* (Springer, 2020), pp. 1–48.
32. W. Liao, Z. Hua, C. Liu, L. Lin, R. Chen, B. Hou, Characterization of T-dependent and T-independent B cell responses to a virus-like particle. *J. Immunol.* **198**, 3846–3856 (2017).
33. J. R. Adams, S. L. Haughney, S. K. Mallapragada, Effective polymer adjuvants for sustained delivery of protein subunit vaccines. *Acta Biomater.* **14**, 104–114 (2015).
34. P. R. Mittelstadt, A. L. DeFranco, Induction of early response genes by cross-linking membrane Ig on B lymphocytes. *J. Immunol.* **150**, 4822–4832 (1993).
35. M. F. A. Woodruff, B. Reid, K. James, Effect of antilymphocytic antibody and antibody fragments on human lymphocytes in vitro. *Nature* **215**, 591–594 (1967).
36. W. Liu, Y.-H. Chen, High epitope density in a single protein molecule significantly enhances antigenicity as well as immunogenicity: A novel strategy for modern vaccine development and a preliminary investigation about B cell discrimination of monomeric proteins. *Eur. J. Immunol.* **35**, 505–514 (2005).
37. J. J. Moon, H. Suh, A. V. Li, C. F. Ockenhouse, A. Yadava, D. J. Irvine, Enhancing humoral responses to a malaria antigen with nanoparticle vaccines that expand T_{fh} cells and promote germinal center induction. *Proc. Natl. Acad. Sci. U.S.A.* **109**, 1080–1085 (2012).
38. S. R. Little, Reorienting our view of particle-based adjuvants for subunit vaccines. *Proc. Natl. Acad. Sci. U.S.A.* **109**, 999–1000 (2012).
39. Z. R. Zacharias, K. A. Ross, E. E. Hornick, J. T. Goodman, B. Narasimhan, T. J. Waldschmidt, K. L. Legge, Polyanhydride nanovaccine induces robust pulmonary B and T cell immunity and confers protection against homologous and heterologous influenza A virus infections. *Front. Immunol.* **9**, 1953 (2018).
40. H. H. Wortis, M. Teutsch, M. Higer, J. Zheng, D. C. Parker, B-cell activation by crosslinking of surface IgM or ligation of CD40 involves alternative signal pathways and results in different B-cell phenotypes. *Proc. Natl. Acad. Sci. U.S.A.* **92**, 3348–3352 (1995).
41. S. A. Haxhinasto, G. A. Bishop, Synergistic B cell activation by CD40 and the B cell antigen receptor: Role of B lymphocyte antigen receptor-mediated kinase activation and tumor necrosis factor receptor-associated factor regulation. *J. Biol. Chem.* **279**, 2575–2582 (2004).
42. J. S. Rush, P. D. Hodgkin, B cells activated via CD40 and IL-4 undergo a division burst but require continued stimulation to maintain division, survival and differentiation. *Eur. J. Immunol.* **31**, 1150–1159 (2001).
43. J. Lee, P. Sengupta, J. Brzostowski, J. Lippincott-Schwartz, S. K. Pierce, The nanoscale spatial organization of B-cell receptors on immunoglobulin M- and G-expressing human B-cells. *Mol. Biol. Cell* **28**, 511–523 (2017).
44. R. Veneziano, T. J. Moyer, M. B. Stone, E. C. Wamhoff, B. J. Read, S. Mukherjee, T. R. Shepherd, J. Das, W. R. Schief, D. J. Irvine, M. Bathe, Role of nanoscale antigen organization on B-cell activation probed using DNA origami. *Nat. Nanotechnol.* **15**, 716–723 (2020).
45. Z. Wan, X. Chen, H. Chen, Q. Ji, Y. Chen, J. Wang, Y. Cao, F. Wang, J. Lou, Z. Tang, W. Liu, The activation of IgM- or isotype-switched IgG- and IgE-BCR exhibits distinct mechanical force sensitivity and threshold. *eLife* **4**, e06925 (2015).
46. J. J. Taylor, K. A. Pape, H. R. Steach, M. K. Jenkins, Apoptosis and antigen affinity limit effector cell differentiation of a single naïve B cell. *Science* **347**, 784–787 (2015).
47. N. A. Buss, S. J. Henderson, M. McFarlane, J. M. Shenton, L. de Haan, Monoclonal antibody therapeutics: History and future. *Curr. Opin. Pharmacol.* **12**, 615–622 (2012).
48. M. Marovich, J. R. Mascola, M. S. Cohen, Monoclonal antibodies for prevention and treatment of COVID-19. *JAMA* **324**, 131–132 (2020).
49. M. Tuccori, S. Ferraro, I. Convertino, E. Cappello, G. Valdiserra, C. Blandizzi, F. Maggi, D. Focosi, Anti-SARS-CoV-2 neutralizing monoclonal antibodies: Clinical pipeline. *MAbs* **12**, 1854149 (2020).
50. M. Pihlgren, A. B. Silva, R. Madani, V. Giriens, Y. Waeckerle-Men, A. Fettelschoss, D. T. Hickman, M. P. López-Deber, D. M. Ndao, M. Vukicevic, A. L. Buccarello, V. Gafner, N. Chuard, P. Reis, K. Piorkowska, A. Pfeifer, T. M. Kündig, A. Muhs, P. Johansen, TLR4- and TRIF-dependent stimulation of B lymphocytes by peptide liposomes enables T cell-independent isotype switch in mice. *Blood* **121**, 85–94 (2013).
51. K. Ross, J. Adams, H. Loyd, S. Ahmed, A. Sambol, S. Broderick, K. Rajan, M. Kohut, T. Bronich, M. J. Wannemuehler, S. Carpenter, S. Mallapragada, B. Narasimhan, Combination nanovaccine demonstrates synergistic enhancement in efficacy against influenza. *ACS Biomater Sci. Eng.* **2**, 368–374 (2016).
52. K. Ross, S. Senapati, J. Alley, R. Darling, J. Goodman, M. Jefferson, M. Uz, B. Guo, K. J. Yoon, D. Verhoeven, M. Kohut, S. Mallapragada, M. Wannemuehler, B. Narasimhan, Single dose combination nanovaccine provides protection against influenza A virus in young and aged mice. *Biomater. Sci.* **7**, 809–821 (2019).
53. D. A. Wagner, S. M. Kelly, A. C. Petersen, N. Peroutka-Bigus, R. J. Darling, B. H. Bellaire, M. J. Wannemuehler, B. Narasimhan, Single-dose combination nanovaccine induces both rapid and long-lived protection against pneumonic plague. *Acta Biomater.* **100**, 326–337 (2019).

Acknowledgments: B.N. is grateful to the Vlasta Klima Balloun Faculty Chair, and S.K.M. is grateful to the Carol Vohs Johnson Chair. **Funding:** We acknowledge financial support from NIH-NIAID (R01 AI141196 and R01 AI154458). B.N. and S.S. acknowledge partial support from NIH-NIAID (R01 AI127565). We also acknowledge support from the Iowa State University Nanovaccine Institute. **Author contributions:** S.S., R.J.D., M.J.W., B.N., and S.K.M. contributed to conception and design of the experiments. S.S. and R.J.D. contributed to the execution of in vitro studies, and S.S. and K.A.R. carried out the in vivo studies. S.S., R.J.D., K.A.R., M.J.W., B.N., and S.K.M. were involved in drafting, revising, and approval of the final version of the manuscript. **Competing interests:** B.N. and M.J.W. are co-founders of ImmunoNanoMed Inc., a start-up with business interests in the development of nano-based vaccines against infectious diseases. B.N. also has a financial interest in Degimflex LLC. S.K.M. is a co-founder of Degimflex LLC., a start-up with business interests in the development of flexible degradable electronic films for biomedical applications. She also has a financial interest in ImmunoNanoMed Inc. S.S., M.J.W., B.N., and S.K.M. are co-inventors on a patent application related to this work filed by Iowa State University Research Foundation (no. PCT/US21/36436, filed on 8 June 2021). S.K.M. is a co-inventor on a currently licensed patent related to this work awarded to the Iowa State University Research Foundation (U.S. Patent no. 7,217,776, 15 May 2007). The authors declare no other competing interests. **Data and materials availability:** All data needed to evaluate the conclusions in the paper are present in the paper and/or the Supplementary Materials. The PBCs can be provided by S.K.M. pending scientific review and a completed material transfer agreement. Requests for the PBCs should be submitted to S.K.M.

Submitted 24 April 2021
Accepted 17 June 2021
Published 4 August 2021
10.1126/sciadv.abj1691

Citation: S. Senapati, R. J. Darling, K. A. Ross, M. J. Wannemeuhler, B. Narasimhan, S. K. Mallapragada, Self-assembling synthetic nanoadjuvant scaffolds cross-link B cell receptors and represent new platform technology for therapeutic antibody production. *Sci. Adv.* **7**, eabj1691 (2021).

Downloaded from http://advances.sciencemag.org/ on August 11, 2021

Science Advances

Self-assembling synthetic nanoadjuvant scaffolds cross-link B cell receptors and represent new platform technology for therapeutic antibody production

Sujata Senapati, Ross J. Darling, Kathleen A. Ross, Michael J. Wannemeuhler, Balaji Narasimhan and Surya K. Mallapragada

Sci Adv **7** (32), eabj1691.
DOI: 10.1126/sciadv.abj1691

ARTICLE TOOLS http://advances.sciencemag.org/content/7/32/eabj1691

SUPPLEMENTARY MATERIALS http://advances.sciencemag.org/content/suppl/2021/08/02/7.32.eabj1691.DC1

REFERENCES This article cites 52 articles, 13 of which you can access for free
http://advances.sciencemag.org/content/7/32/eabj1691#BIBL

PERMISSIONS http://www.sciencemag.org/help/reprints-and-permissions

Use of this article is subject to the Terms of Service

Science Advances (ISSN 2375-2548) is published by the American Association for the Advancement of Science, 1200 New York Avenue NW, Washington, DC 20005. The title *Science Advances* is a registered trademark of AAAS.

Copyright © 2021 The Authors, some rights reserved; exclusive licensee American Association for the Advancement of Science. No claim to original U.S. Government Works. Distributed under a Creative Commons Attribution NonCommercial License 4.0 (CC BY-NC).

Downloaded from http://advances.sciencemag.org/ on August 11, 2021